

# Harnessing magnetic anisotropy for nonlinear magnetization precession and spin waves

P. I. Gerevenkov,<sup>1,\*</sup> L. A. Shelukhin,<sup>1</sup> Ia. A. Filatov,<sup>1</sup> P. A. Dvortsova,<sup>1</sup> and A. M. Kalashnikova<sup>1</sup>

<sup>1</sup>*Ioffe Institute, 194021 St. Petersburg, Russia*

The nonlinearity of magnetization precession and spin waves is a cornerstone of contemporary magnonics. We investigate nonlinear magnetization dynamics in a thin epitaxial iron film driven by femtosecond laser pulses in regimes of homogeneous precession and propagating magnetostatic spin wave packets. The magnetization precession anharmonicity, the generation of higher-order harmonics, and the dynamical rectification are experimentally demonstrated. The numerical solution of the non-linearized Landau-Lifshitz-Gilbert equation reveals that these effects stem from the asymmetry in the energy potential. This asymmetry is readily achievable when an external magnetic field with a strength comparable to the magnetic anisotropy field is applied close to the hard axis. This work establishes a connection between the geometry of the energy profile and nonlinear responses, paving the way for designing magnonic devices with controlled harmonic generation and nonlinear spin wave interaction.

In wave physics, nonlinearity is traditionally understood as a wave-induced change in a medium's parameters (such as dispersion, damping, etc.) that allows waves to interact [3]. The study of such interactions in magnetic systems is crucial for applications ranging from all-magnonic transistors [4, 5] to computing [6], neuromorphic devices [7, 8], and frequency-comb generation [9–12]. Within the macrospin approximation – setting aside processes like the splitting of one oscillation into several [13–15] – research is largely focused on the type-I Suhl nonlinearity, which involves a change in the demagnetizing fields due to the reduction of the longitudinal effective field component of magnetization during large-angle precession [16–20]. Here, the onset of nonlinearity is typically linked to high-amplitude precessions or waves, while specific physical mechanisms behind the nonlinearity are often not detailed. Conventionally, the nonlinear regime is identified through a shift in resonant frequency [19, 21–23] or the generation of higher harmonics [24–28]. However, at large amplitudes and pronounced ellipticity of precession, the generation of a second harmonic of a purely geometric nature occurs [29–31]. In this case, only the double frequency can be generated, and the waves may not interact if the dispersion relation remains amplitude-independent [32].

In this Letter, we examine a general mechanism that exploits the asymmetric energy potential created by a magnetic field and magnetic anisotropy, leading directly to nonlinear magnetization precession. This mechanism allowed us to experimentally demonstrate the generation of higher harmonics up to the 4th order, a magnetization precession rectification effect, and a nonlinear shift of the resonance frequency for both uniform magnetization precession and spin wave packets in a thin film of the ferromagnet Fe. The proposed mechanism is not reducible to type-I Suhl nonlinearity and is observed for magnetization deviations from equilibrium of less than one degree.

We employed the time-resolved magneto-optical Kerr effect to study magnetization dynamics in a thin ferromagnetic metallic film. An epitaxial Fe (001) film with a thickness  $d = 20$  nm grown by pulsed laser deposition on a MgO (001) substrate [33, 34] exhibits cubic magnetocrystalline anisotropy in the plane, with easy axes along the  $\langle 110 \rangle$  MgO directions [inset in Fig. 1(a)]. External magnetic field ( $\mathbf{H}_{ext}$ ) is applied in the film plane and makes an angle  $\phi_H$  with the anisotropy hard axis (HA). Ultrafast heating by a 190-fs laser pulse rapidly reduces the effective anisotropy field through demagnetization and a change in the magnetic anisotropy parameter [35]. As a result, magnetization precession is triggered within the volume excited by the pump pulse, and its frequency is controlled by the effective magnetic anisotropy field altered by the optical excitation [36, 37]. Additionally, a magnetostatic wavepacket is launched and propagates laterally away from the laser spot according to the dispersion governed by the equilibrium anisotropy and  $\mathbf{H}_{ext}$  [38, 39]. To monitor laser-induced precession and wavepackets, time- and spatially resolved magneto-optical pump-probe measurements were performed as described elsewhere [38] and in Sec. I of Suppl. Material [40]. To analyze magnetization precession and spin waves and to comprehend the features of nonlinear behaviour, we used a numerical solution of the non-linearized Landau-Lifshitz-Gilbert (LLG) equation in the time domain, as well as micromagnetic simulations in mumax3 [41] that included the time-dependent and spatially localized change of magnetization and magnetic anisotropy parameters.

Characterization of the magnetic parameters of the film was performed by measuring the azimuthal dependence of laser-induced precession of magnetization in a relatively strong applied field  $\mu_0 H_{ext} = 100$  mT, preventing any pronounced nonlinearity (for details of the procedure see [37]). The following equilibrium parameters of the film were obtained. Saturation magnetization is  $M_S = 1.9 \text{ MA m}^{-1}$ , and the cubic anisotropy parameter is  $K_C = 59.5 \text{ kJ m}^{-3}$ . Importantly, the film demonstrated Gilbert damping  $\alpha_G = 2.5 \cdot 10^{-3}$  which is comparable to the lowest damping parameters reported

\* petr.gerevenkov@mail.ioffe.ru; <http://www.ioffe.ru/ferrolab/>

for epitaxial Fe films at room temperature [42], that is crucial for reliable demonstration of nonlinearities in both magnetization precession and spin waves. Using the same results, the impact of the laser pulse on magnetic parameters was quantified yielding demagnetization by 6 % and a decrease in  $K_C$  by 45 % according to a power law  $(K_C(T)/K_C(0)) = (M_S(T)/M_S(0))^{10}$  [37, 43] at the pump area center and for a mean fluence of  $F = 14 \text{ mJ}\cdot\text{cm}^{-2}$ . The changes of  $M_S$  and  $K_C$  were assumed to be instantaneous with relaxation times of 1.55 ns.

To explore the nonlinear precession and spin waves we rely on an interplay between magnetic anisotropy and  $\mathbf{H}_{ext}$  that shapes the magnetic energy profile in a ferromagnet. In particular, when a magnetic field is applied close to the HA and has a value close to the effective anisotropy field, the free energy profile becomes intrinsically nonsymmetric and nonparabolic, that favours nonlinearity. Thus, for a nonlinear magnetization precession, we design the experiment such that this condition is met when the magnetization and anisotropy are reduced by a laser pulse. We direct the applied field  $\mu_0 H_{ext} = 40 \text{ mT}$  at an angle  $\phi_H = 2.5^\circ$  to the HA [inset in Fig. 1 (a)]. Using the magnetic parameters altered by a laser pulse, we calculated the temporal evolution of magnetization within a macrospin approach. The out-of-plane component of magnetization is shown in Fig. 1 (a) by a red line. The signal clearly differs from a damped sine-like function [black dashed line in the Fig. 1 (a)], indicating precession anharmonicity and signifying its nonlinear origin [44]. The FFT frequency spectrum of the data exhibits both the fundamental mode of precession (marked as FMR) and peaks corresponding to its higher harmonics up to the 4th [red line in Fig. 1 (b)].

To confirm that such pronounced nonlinearity in time and frequency domains can be observed experimentally, we plot in Fig. 1(a, b) the signal obtained with the weakly-focused, spatially-overlapped pump and probe pulses [40] and its FFT. The laser fluence was chosen to achieve the same reduction of the magnetic parameters as in the calculations. There is a striking agreement between the calculated and experimental curves exhibiting the very same features. Note that equidistant peaks in the FFT spectrum rule out thickness spin-wave resonance – which has a quadratically distributed spectrum with mode number – as the source of the anharmonicity [45, 46]. Also, the 1st-order spin-wave resonance for a 20-nm-thick iron film is at 85 GHz, which is significantly higher than all observed harmonics.

To reveal under which conditions nonlinearity is the most pronounced, we plot in Fig. 1(c) the FMR frequency dependence on the external magnetic field obtained in experiment (symbols) and in numerical calculations (red solid line) that are in good agreement with each other. In contrast, near the critical field of the laser-excited film (40 mT) the solution of the linearized LLG equation (black dashed line) does not match the experimental results. Also, higher harmonics appear in the

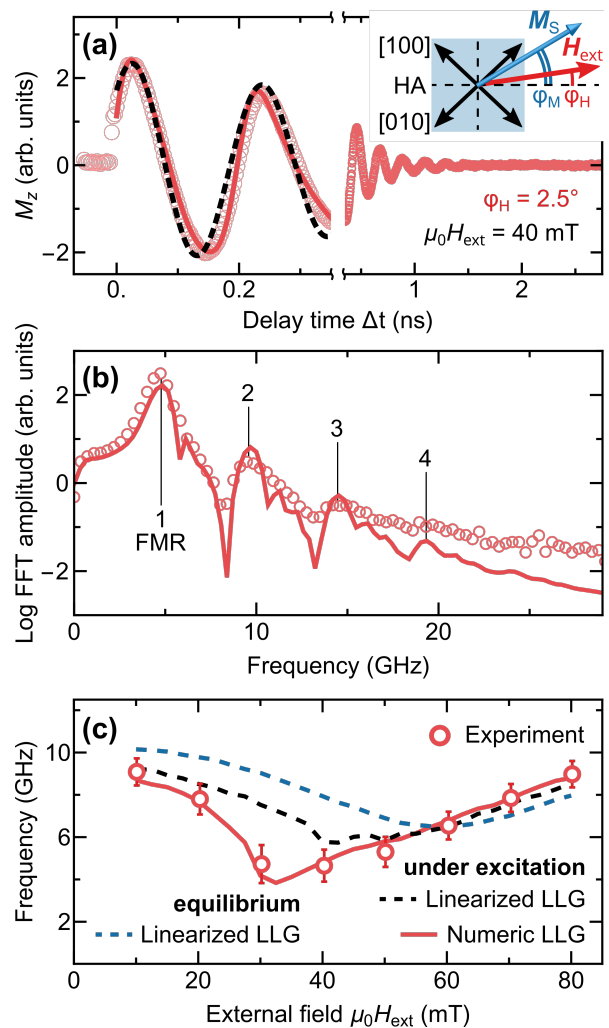


**FIG. 1. Anharmonicity and higher harmonics generation.** (a) Experimental pump-probe signals, proportional to the out-of-plane magnetization component (points). The measurements are performed in the field  $\mu_0 H_{ext} = 40 \text{ mT}$ , directed at an angle  $\phi_H = 2.5^\circ$ . The solid red and dashed black lines correspond to the numerical LLG solution and single frequency damped sine, respectively. Insert in (a) shows a sketch of the anisotropy axes in the plane of the film and the angles designations. Easy axes are shown by the double-headed arrows, hard axes – by the dashed lines. (b) FFT of the experimental signals and the numeric LLG solution from (a). The observed harmonics are numbered (1 corresponds to the eigen frequency). (c) Field dependencies of the experimental eigen frequency (points), numeric (solid red line) and linearized (dashed black line) LLG solutions. Error bars show the standard deviation of the experimental FFT peaks.

same field region. Importantly, nonlinearity causes qualitative changes in the field dependence of the FMR frequency that can not be explained by only laser-induced reduction of  $M_S$  and  $K_C$ . To emphasise it, we plot in Fig. 1(c) the solution of the linearized LLG for the equilibrium parameters of the film (dashed blue line). Clearly, disregarding nonlinearity can obscure the conclu-

sions regarding the laser-induced changes of a magnetic state.

In order to understand the physical mechanism behind the higher harmonics of the precession, we plot in Fig. 2 (a) the energy profile in the sample plane as a function of the in-plane magnetization angle  $\phi_M$  [see inset in Fig. 1 (a)] calculated under the laser excitation (red line), as well as for the equilibrium film (blue line). The field of  $\mu_0 H_{ext} = 30$  mT was chosen, as it corresponds to the largest frequency shift in Fig. 1 (c). Calculations confirm that the potential energy in the film plane becomes asymmetric under laser excitation. Magnetization precession in such a non-parabolic energy potential leads to the appearance of both odd and even harmonics with the same polarization as the fundamental mode.

In the case of zero damping, the precession follows an isoenergetic trajectory, since the LLG equation lacks inertial terms. This results in a highly non-elliptical magnetization trajectory [presented in Fig. 2 (b) in terms of out-of-plane  $\phi_M^{oop}$  and in-plane  $\phi_M^{ip}$  magnetization angles]. Notably, the trajectory has a mirror symmetry only in the out-of-plane direction, signifying that the pronounced shape anisotropy leads to a parabolic energy profile in the direction normal to the film plane and to a strong ellipticity. By aligning the major axis of the precession trajectory with the direction of potential asymmetry, the nonlinearity can be significantly enhanced.

We also obtain magnetic rectification manifesting itself as the discrepancy between the period-averaged magnetization orientation  $\phi_{\langle M \rangle}$  and the energy minimum after laser excitation  $\phi_M^{min}$  [solid black and open red dots in Fig. 2 (a,b), respectively]. This resembles the effect of thermal expansion of solids [47]. When an external field  $\mathbf{H}_{ext}$  with a strength comparable to the anisotropy field is applied close to the hard axis, it reduces the barrier between the two equivalent anisotropy energy minima at  $\pm\phi_M^{min}$ . Small in-plane deviation of  $\mathbf{H}_{ext}$  from the hard axis lifts the equivalence between the two minima. Rectification shifts  $\phi_{\langle M \rangle}$  toward the flatter slope of the potential, i.e., toward the HA. This leads to a reduction in the precession frequency, compared to the linear theoretical predictions [Fig. 1 (c)].

To discuss magnetization precession with non-zero damping, we introduce the time-dependent magnetic rectification as  $R(\Delta t) = \phi_{\langle M \rangle}(\Delta t) - \phi_M^{min}$  and the instantaneous amplitude in the sample plane  $A_{ins}^{ip}(\Delta t)$  as half of the peak-to-peak value over the precession period [Fig. 2 (b)]. In this case, the magnetization follows a spiral trajectory towards equilibrium [black dashed lines in Fig. 2 (a)]. Multiple precession cycles can be approximated by precession periods with zero damping and varying amplitudes. For a fixed  $\phi_H$ , material parameters, and pump fluence, the maximum rectification  $R^{max}$  right after the excitation can be presented as a function of the  $\mathbf{H}_{ext}$  value [Fig. 2 (c)]. In the case of finite damping, the rectification  $R(\Delta t)$  decreases with the precession amplitude  $A_{ins}^{ip}$  but persists until the magnetization dynamics

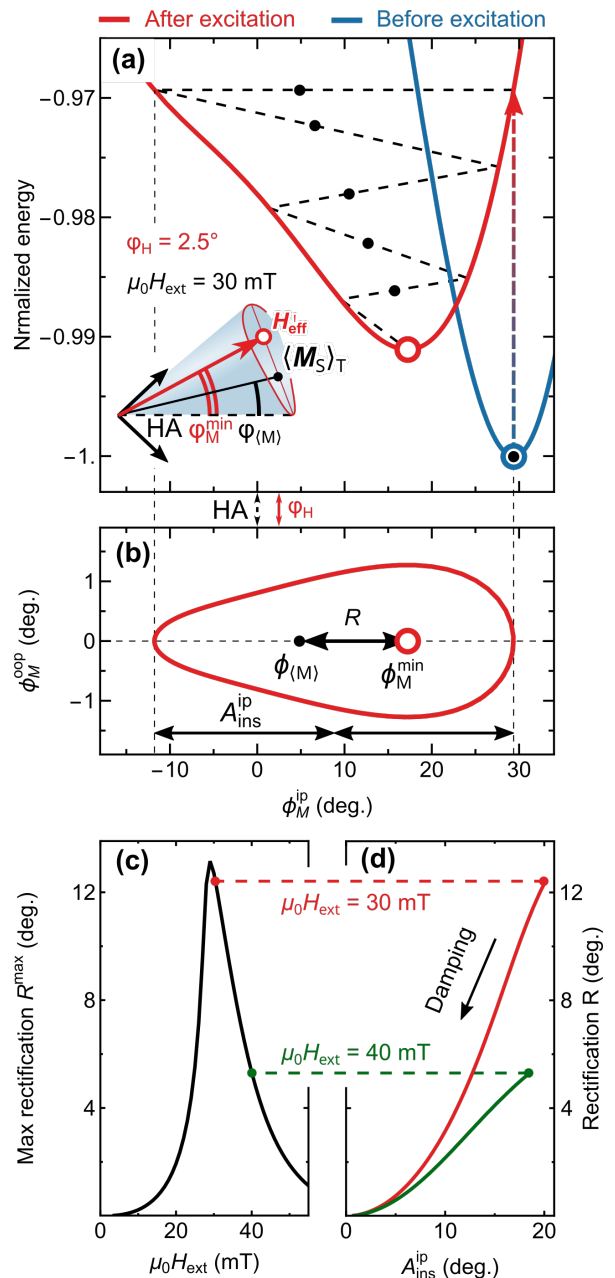


FIG. 2. **Energy profile asymmetry as a source of anharmonicity.** (a) Energy as a function magnetization direction in the film plane  $\phi_M^{ip}$  before (blue line) and after (red line) excitation by a femtosecond laser pulse. The dashed black line is a sketch illustrating the in-plane deviation change during the damping process. (b) Trajectory of magnetization precession in coordinates deviation in-plane – deviation out-of-plane of the film. Empty points show positions of the energy minima. Black points correspond to the mean magnetization direction ( $\phi_{\langle M \rangle}$ ) over the precession period. (c) Dependence of rectification  $R = \phi_{\langle M \rangle} - \phi_M^{min}$  on the external magnetic field at zero Gilbert damping. (d) Dependence of  $R$  on the precession amplitude during the damping process for external magnetic field values of  $\mu_0 H_{ext} = 30$  (red) and 40 mT (green).

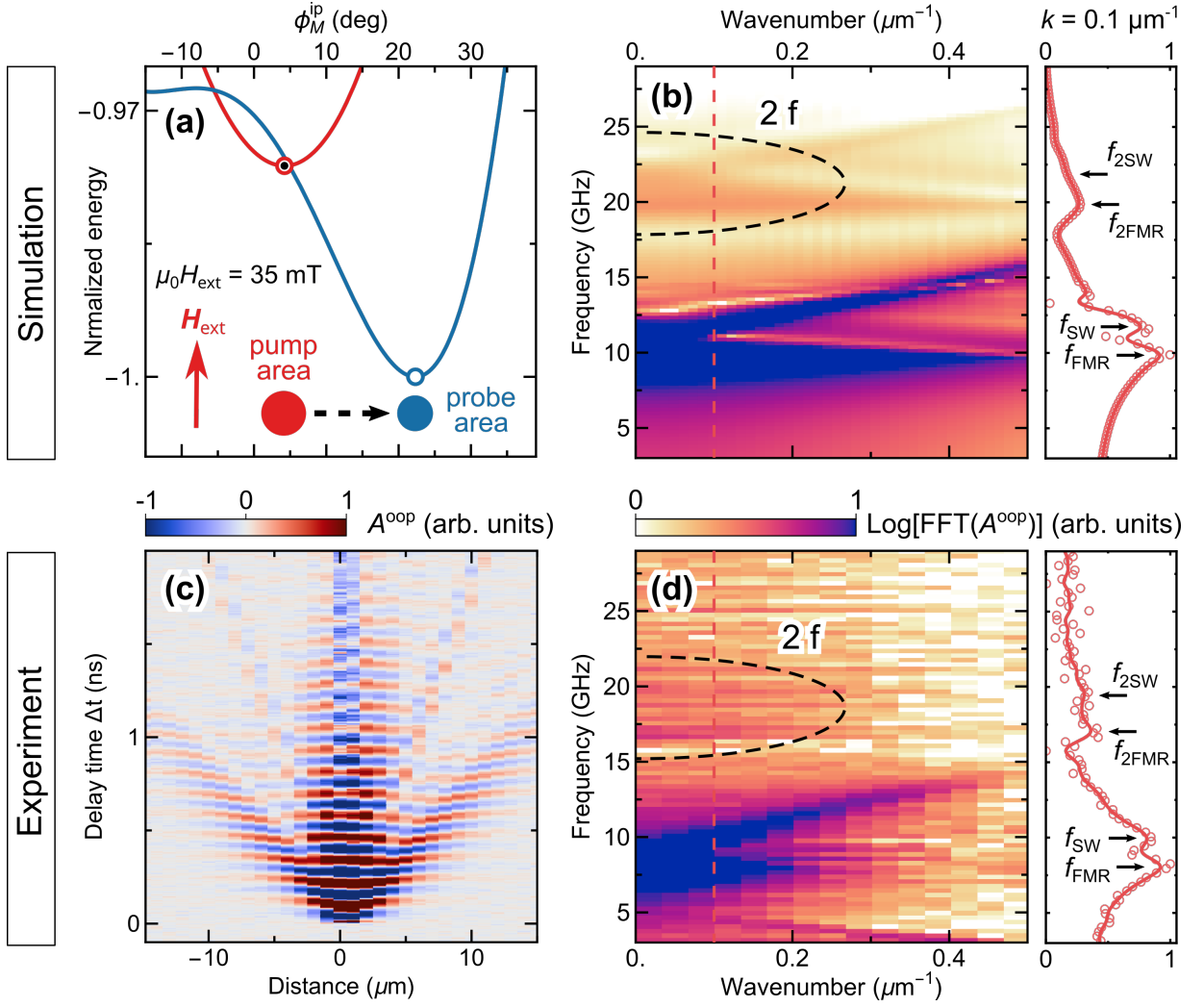


FIG. 3. **The second harmonic of a propagating magnetostatic wave.** (a) Dependence of energy vs. magnetization direction in the film plane inside (red) and outside (blue) the excitation area at  $\mu_0 H_{ext} = 35$  mT. (c) Map of pump-probe signal vs distance and delay time ( $\Delta t$ ) between excitation and detection. The measurements performed in the field  $\mu_0 H_{ext} = 35$  mT, directed at an angle  $\phi_H$  of  $2.5^\circ$  in the Damon-Eshbach geometry. (b,d) 2D FFT of the experimental data (d) and the data, obtained from the micromagnetic simulation at the same parameters (b). The dashed black lines show the second harmonic of the magnetization dynamics. The panels on the right show cross-sections of the corresponding maps at  $k = 0.1 \mu\text{m}^{-1}$  with a guide to the eyes (solid line). The cross-section are marked with a red dashed line on the maps. The arrows on the cross-sections indicate the peaks of the spectral amplitudes corresponding to the first and second harmonics of the FMR and SSW.

is fully attenuated, indicating the absence of a threshold [see Fig. 2 (d)].

The pronounced nonlinearity allows us to observe the effect even at low amplitudes, including the case of propagating magnetostatic waves. Indeed, let's consider the potential inside and outside the excitation region [red and blue lines in Fig. 3 (b), respectively]. After excitation, the wave propagates into regions of the film characterized by equilibrium parameters. If potential asymmetry exists in the region of the film where the wave propagates, the latter should exhibit nonlinear properties.

We test this by generating the second harmonic of a wavepacket of magnetostatic surface spin waves (SSW) propagating perpendicular to  $\mathbf{H}_{ext}$  [see inset in

Fig. 3 (a)]. First, we carried out a micromagnetic simulation (Sec. II in Supp. Mater. [40]). The laser-induced change of  $M_S$  and  $K_C$  are 25% and 94%, respectively, corresponding to a mean laser fluence of  $F = 39 \text{ mJ}\cdot\text{cm}^{-2}$ . To achieve an asymmetric energy potential in the unexcited region at  $\phi_H = 2.5^\circ$ , the field value was set to  $\mu_0 H_{ext} = 35$  mT [Fig. 3 (a)]. Note that this geometry provides the longest propagation distance for the SSW packets [38]. Calculated spatial-temporal maps (see details in Sec. II Suppl. Material [40]) were used to obtain the SSW dispersion. The dispersion in Fig. 3 (b) shows a propagating SSW along with the wave at the doubled frequency (encompassed by the black dashed line). At  $k = 0.1 \mu\text{m}^{-1}$ , peaks corresponding to the FMR, SSW,

and their doubled frequencies are visible [right side of Fig. 3 (b)]. The second harmonic signal propagates at the same speed as the fundamental wave packet of the SSW (see the slope of the lines). This confirms anharmonicity as a mechanism of nonlinearity – the first and second harmonics are inseparable in space and time.

The same conditions were reproduced in the experiment. The spatial-temporal map of the magneto-optical response shows propagating SSW packets [Fig. 3 (c)]. A two-dimensional Fourier transform of the data reveals the wave dispersion [Fig. 3 (d)]. The second harmonic of the SSW packet was also observed. However, the signal-to-noise ratio is insufficient to confirm its propagation via group velocity (i.e. the dispersion slope). Nevertheless, in the cross-section at  $k = 0.1 \mu\text{m}^{-1}$ , a peak at the doubled frequency of the SSW is visible [right side of Fig. 3 (d)] in good agreement with the simulation results. Subtracting the signal from the central region confirms the double-frequency signal beyond the excitation area (see details in Sec. III Suppl. Material [40]). This indicates the propagation of the second harmonic at the same group velocity as the SSW. It is also worth noting that the SSW carries a rectified in-plane component, as the trajectory of the local magnetic moments resembles the one shown in Fig. 2 (b). The existence of rectification over the entire range of amplitudes [Fig. 2 (d)] allows such waves to interact nonlinearly [3].

In summary, we have experimentally demonstrated an intrinsic nonlinear mechanism in magnetization dynamics. If an external magnetic field is close to the hard axis of a magnetic specimen and its value is close to the anisotropy field, the energy profile around the global minimum becomes asymmetric. This asymmetry arises from the nearby local energy minima. As a result, the dynamics becomes intrinsically nonlinear. This also implies that the Landau-Lifshitz-Gilbert equation cannot be linearized under these conditions, even for small am-

plitudes. The magnetization dynamics exhibit three effects: anharmonicity of magnetization precession, which deviates from a single-frequency damped harmonic function; generation of odd and even higher harmonics of the magnetization dynamics; qualitative deviation of the fundamental precession mode frequency from the linear theory prediction. The latter is understood based on the magnetic rectification effect, which causes magnetization to oscillate around a point distinct from the energy minimum.

The presence of the effect at small deviations of magnetization makes it possible to excite nonlinear propagating wave packets of spin waves that do not require high excitation power. Our results establish a direct link between the magnetic energy landscape and nonlinear responses. This understanding provides a pathway for designing magnonic and spintronic devices whose operation relies on controlled harmonic generation and interaction between spin waves. The demonstrated nonlinearities only require properly tailored magnetic anisotropy of a medium in combination with an external magnetic field or, more generally, other fields with the same symmetry, e.g. an exchange bias field. While we used laser-induced ultrafast heating to trigger the nonlinear magnetization dynamics, there is no restriction regarding an excitation method, and one envisages exploiting various ultrafast opto-magnetic effects [48] and even nonoptical excitation approaches [20, 49]. In ultrafast magnetism, our results have direct implications, as the laser-driven tuning of the precession frequency is one of the goals [49–51], and also serves as a probe of the magnetic state following THz, infrared, and optical excitations [36, 37, 51–56].

The work of P.I.G. on pump-probe experiments, theoretical analysis, and micromagnetic simulations was supported by the grant of the RSF No. 24-72-00136, <https://rscf.ru/project/24-72-00136/>.

- 
- [1] R. Boyd, *Nonlinear Optics* (Elsevier Science, 2020).
  - [2] I. A. Filatov, P. I. Gerevenkov, A. V. Azovtsev, V. A. Kovaleva, N. E. Khokhlov, and A. M. Kalashnikova, Magnon-cherenkov effect from a picosecond strain pulse, *Nature Physics* 10.1038/s41567-025-03137-8 (2026).
  - [3] D. Breitbach, M. Bechberger, B. Heinz, A. Hamadeh, J. Maskill, K. O. Levchenko, B. Lagel, C. Dubs, Q. Wang, R. Verba, *et al.*, Nonlinear erasing of propagating spin-wave pulses in thin-film ga: Yig, *Applied Physics Letters* **124**, 10.1063/5.0189648 (2024).
  - [4] A. V. Chumak, A. A. Serga, and B. Hillebrands, Magnon transistor for all-magnon data processing, *Nature communications* **5**, 4700 (2014).
  - [5] X. Ge, R. Verba, P. Pirro, A. V. Chumak, and Q. Wang, Nanoscaled magnon transistor based on stimulated three-magnon splitting, *Applied Physics Letters* **124**, 10.1063/5.0189619 (2024).
  - [6] Q. Wang, M. Kewenig, M. Schneider, R. Verba, F. Kohl, B. Heinz, M. Geilen, M. Mohseni, B. Lagel, F. Ciubotaru, C. Adelmann, C. Dubs, S. D. Cotozana, O. V. Dobrovolskiy, T. Bracher, P. Pirro, and A. V. Chumak, A magnonic directional coupler for integrated magnonic half-adders, *Nature Electronics* **3**, 765–774 (2020).
  - [7] A. Papp, W. Porod, and G. Csaba, Nanoscale neural network using non-linear spin-wave interference, *Nature Communications* **12**, 10.1038/s41467-021-26711-z (2021).
  - [8] A. Lutsenko, K. G. Fripp, L. Flajšman, A. V. Shytov, V. V. Kruglyak, and S. van Dijken, Non-linear dynamics in magnonic fabry-p\{e} rot resonators: Low-power neuron-like activation and transmission suppression, *arXiv preprint arXiv:2602.10650* 10.48550/arXiv.2602.10650 (2026).
  - [9] C. Wang, J. Rao, Z. Chen, K. Zhao, L. Sun, B. Yao, T. Yu, Y.-P. Wang, and W. Lu, Enhancement of magnonic frequency combs by exceptional points, *Nature Physics* **20**, 1139 (2024).
  - [10] Z. Wang, H. Yuan, Y. Cao, Z.-X. Li, R. A. Duine, and P. Yan, Magnonic frequency comb through nonlin-

- ear magnon-skyrmion scattering, *Physical Review Letters* **127**, 037202 (2021).
- [11] Y. Khivintsev, J. Marsh, V. Zagorodnii, I. Harward, J. Lovejoy, P. Krivosik, R. Camley, and Z. Celinski, Nonlinear amplification and mixing of spin waves in a microstrip geometry with metallic ferromagnets, *Applied Physics Letters* **98**, 10.1063/1.3541787 (2011).
- [12] X. Guo, T. Gong, G. Lan, M. Guo, X. Han, G. Yu, P. Yan, and Q. Wang, Stimulated magnonic frequency combs, arXiv preprint arXiv:2601.21370 10.48550/arXiv.2601.21370 (2026).
- [13] R. Dreyer, A. F. Schäffer, H. G. Bauer, N. Liebing, J. Berakdar, and G. Woltersdorf, Imaging and phase-locking of non-linear spin waves, *Nature Communications* **13**, 10.1038/s41467-022-32224-0 (2022).
- [14] V. E. Demidov, H. Ulrichs, S. O. Demokritov, and S. Urazhdin, Nonlinear scattering in nanoscale magnetic elements: Overpopulation of the lowest-frequency magnon state, *Physical Review B—Condensed Matter and Materials Physics* **83**, 020404 (2011).
- [15] S. O. Demokritov, V. E. Demidov, O. Dzyapko, G. A. Melkov, A. A. Serga, B. Hillebrands, and A. N. Slavin, Bose–einstein condensation of quasi-equilibrium magnons at room temperature under pumping, *Nature* **443**, 430 (2006).
- [16] H. Suhl, The theory of ferromagnetic resonance at high signal powers, *Journal of Physics and Chemistry of Solids* **1**, 209 (1957).
- [17] H. Suhl, The nonlinear behavior of ferrites at high microwave signal levels, *Proceedings of the IRE* **44**, 1270 (1956).
- [18] K. Livesey, Nonlinear behavior in metallic thin films and nanostructures, in *Handbook of Surface Science*, Vol. 5 (Elsevier, 2015) pp. 169–214.
- [19] F. Guo, L. M. Belova, and R. D. McMichael, Nonlinear ferromagnetic resonance shift in submicron permalloy ellipses, *Physical Review B* **91**, 064426 (2015).
- [20] B. Flebus, D. Grundler, B. Rana, Y. Otani, I. Barsukov, A. Barman, G. Gubbiotti, P. Landeros, J. Akerman, U. Ebels, *et al.*, The 2024 magnonics roadmap, *Journal of Physics: Condensed Matter* **36**, 363501 (2024).
- [21] Y. Khivintsev, B. Kuanr, T. J. Fal, M. Haftel, R. E. Camley, Z. Celinski, and D. L. Mills, Nonlinear ferromagnetic resonance in permalloy films: A nonmonotonic power-dependent frequency shift, *Phys. Rev. B* **81**, 054436 (2010).
- [22] M. Wismayer, B. Southern, X. Fan, Y. Gui, C.-M. Hu, and R. Camley, Nonlinear behavior for the uniform mode and horizontal standing spin-wave modes in metallic ferromagnetic microstrips: Experiment and theory, *Physical Review B—Condensed Matter and Materials Physics* **85**, 064411 (2012).
- [23] E. Edwards, H. Ulrichs, V. Demidov, S. Demokritov, and S. Urazhdin, Parametric excitation of magnetization oscillations controlled by pure spin current, *Physical Review B—Condensed Matter and Materials Physics* **86**, 134420 (2012).
- [24] Z. Zhang, F. Sekiguchi, T. Moriyama, S. C. Furuya, M. Sato, T. Satoh, Y. Mukai, K. Tanaka, T. Yamamoto, H. Kageyama, *et al.*, Generation of third-harmonic spin oscillation from strong spin precession induced by terahertz magnetic near fields, *Nature Communications* **14**, 1795 (2023).
- [25] J. Marsh, V. Zagorodnii, Z. Celinski, and R. Camley, Nonlinearly generated harmonic signals in ultra-small waveguides with magnetic films: Tunable enhancements of 2nd and 4th harmonics, *Applied Physics Letters* **100**, 10.1063/1.3688036 (2012).
- [26] W. He, B. Hu, Q.-F. Zhan, X.-Q. Zhang, and Z.-H. Cheng, Probing nonlinear magnetization dynamics in fe/mgo (001) film by all optical pump-probe technique, *Applied Physics Letters* **104**, 10.1063/1.4871006 (2014).
- [27] C. Cheng and W. E. Bailey, High-efficiency gigahertz frequency doubling without power threshold in thin-film ni81fe19, *Applied Physics Letters* **103**, 10.1063/1.4842195 (2013).
- [28] M. Hudl, M. d’Aquino, M. Pancaldi, S.-H. Yang, M. G. Samant, S. S. Parkin, H. A. Dürr, C. Serpico, M. C. Hoffmann, and S. Bonetti, Nonlinear magnetization dynamics driven by strong terahertz fields, *Physical review letters* **123**, 197204 (2019).
- [29] P. Solovev, A. Afonin, B. Belyaev, N. Boev, I. Govorun, A. Izotov, A. Ugrymov, and A. A. Leksikov, Second harmonic generation in thin permalloy film, *Journal of Physics D: Applied Physics* **54**, 425002 (2021).
- [30] K. Nikolaev, S. Lake, B. Das Mohapatra, G. Schmidt, S. Demokritov, and V. Demidov, Resonant inter-mode second harmonic generation by backward spin waves in yig nano-waveguides, *Applied Physics Letters* **126**, 10.1063/5.0253293 (2025).
- [31] K. O. Nikolaev, S. Lake, G. Schmidt, S. Demokritov, and V. Demidov, Resonant generation of propagating second-harmonic spin waves in nano-waveguides, *Nature Communications* **15**, 1827 (2024).
- [32] P. Solovev, A. Afonin, B. Belyaev, N. Boev, I. Govorun, A. Izotov, A. Ugrymov, and A. Leksikov, Second harmonic generation as a probe of parametric spin wave instability processes in thin magnetic films, *Physical Review B* **106**, 064406 (2022).
- [33] S. M. Sutorin, P. A. Dvortsova, M. V. Baidakova, M. S. Dunaevskiy, and B. B. Krichevstov, Laser mbe growth of cobalt-platinum multilayers with perpendicular magnetic anisotropy, *Journal of Magnetism and Magnetic Materials* **557**, 169467 (2022).
- [34] P. A. Dvortsova and S. M. Sutorin, Technological peculiarities of epsilon ferrite epitaxial stabilization by pld, *Surfaces* **5**, 445 (2022).
- [35] A. Kalashnikova, N. Khokhlov, L. Shelukhin, and A. Scherbakov, Ultrafast laser-induced control of magnetic anisotropy in nanostructures, *Technical Physics* **68**, 574 (2023).
- [36] E. Carpene, E. Mancini, D. Dazzi, C. Dallera, E. Puppini, and S. De Silvestri, Ultrafast three-dimensional magnetization precession and magnetic anisotropy of a photoexcited thin film of iron, *Physical Review B—Condensed Matter and Materials Physics* **81**, 060415 (2010).
- [37] P. Gerevenkov, D. Kuntu, I. A. Filatov, L. Shelukhin, M. Wang, D. Pattnaik, A. Rushforth, A. Kalashnikova, and N. Khokhlov, Effect of magnetic anisotropy relaxation on laser-induced magnetization precession in thin galfeol films, *Physical Review Materials* **5**, 094407 (2021).
- [38] N. Khokhlov, P. Gerevenkov, L. Shelukhin, A. Azovtsev, N. Pertsev, M. Wang, A. Rushforth, A. Scherbakov, and A. Kalashnikova, Optical excitation of propagating magnetostatic waves in an epitaxial galfeol film by ultrafast magnetic anisotropy change, *Phys. Rev. Appl.* **12**, 044044 (2019).

- [39] I. A. Filatov, P. Gerevenkov, M. Wang, A. Rushforth, A. Kalashnikova, and N. Khokhlov, Spectrum evolution and chirping of laser-induced spin wave packets in thin iron films, *Applied Physics Letters* **120**, 10.1063/5.0077195 (2022).
- [40] See supplemental material at [url will be inserted by publisher] for details of simulation, static magnetisation distribution, and symmetrical propagation of the waves at round spot excitation.
- [41] A. Vansteenkiste, J. Leliaert, M. Dvornik, M. Helsen, F. Garcia-Sanchez, and B. Van Waeyenberge, The design and verification of mumax3, *AIP advances* **4**, 10.1063/1.4899186 (2014).
- [42] B. Khodadadi, A. Rai, A. Sapkota, A. Srivastava, B. Nepal, Y. Lim, D. A. Smith, C. Mewes, S. Budhathoki, A. J. Hauser, *et al.*, Conductivitylike gilbert damping due to intraband scattering in epitaxial iron, *Physical review letters* **124**, 157201 (2020).
- [43] C. Zener, Classical theory of the temperature dependence of magnetic anisotropy energy, *Physical Review* **96**, 1335 (1954).
- [44] A. V. Gaponov-Grekhov and M. I. Rabinovich, Li mandel'shtam and the modern theory of nonlinear oscillations and waves, *Soviet Physics Uspekhi* **22**, 590 (1979).
- [45] R. Weber, Spin-wave resonance, *IEEE Transactions on Magnetics* **4**, 28 (1968).
- [46] M. Seavey Jr and P. Tannenwald, Direct observation of spin-wave resonance, *Phys. Rev. Lett.* **1**, 168 (1958).
- [47] J. S. Dugdale and D. K. C. MacDonald, The thermal expansion of solids, *Physical Review* **89**, 832–834 (1953).
- [48] A. Kimel, A. Kalashnikova, A. Pogrebna, and A. Zvezdin, Fundamentals and perspectives of ultrafast photoferroic recording, *Physics Reports* **852**, 1 (2020).
- [49] A. Barman, G. Gubbiotti, S. Ladak, A. O. Adeyeye, M. Krawczyk, J. Gräfe, C. Adelman, S. Cotofana, A. Naeemi, V. I. Vasyuchka, *et al.*, The 2021 magnonics roadmap, *Journal of Physics: Condensed Matter* **33**, 413001 (2021).
- [50] V. Wiechert, H. Wang, W. Legrand, P. Gambardella, D. Breitbach, P. Pirro, M. Lammel, A. Meo, G. Finocchio, and D. Bossini, On demand laser-induced frequency tuning of coherent magnons in a nanometer-thick magnet at room temperature, *Nature Communications* **17**, 10.1038/s41467-025-66707-7 (2026).
- [51] L. A. Shelukhin, R. R. Gareev, V. Zbarsky, J. Walowski, M. Münzenberg, N. A. Pertsev, and A. M. Kalashnikova, Spin reorientation transition in cofeb/mgo/cofeb tunnel junction enabled by ultrafast laser-induced suppression of perpendicular magnetic anisotropy, *Nanoscale* **14**, 8153–8162 (2022).
- [52] S. Schlauderer, C. Lange, S. Baierl, T. Ebnet, C. P. Schmid, D. Valovcin, A. Zvezdin, A. Kimel, R. Mikhaylovskiy, and R. Huber, Temporal and spectral fingerprints of ultrafast all-coherent spin switching, *Nature* **569**, 383 (2019).
- [53] D. Afanasiev, J. Hortensius, B. Ivanov, A. Sasani, E. Bousquet, Y. M. Blanter, R. V. Mikhaylovskiy, A. V. Kimel, and A. Caviglia, Ultrafast control of magnetic interactions via light-driven phonons, *Nature materials* **20**, 607 (2021).
- [54] L. Soumah, D. Bossini, A. Anane, and S. Bonetti, Optical frequency up-conversion of the ferromagnetic resonance in an ultrathin garnet mediated by magnetoelastic coupling, *Physical Review Letters* **127**, 077203 (2021).
- [55] A. Kuzikova, N. Liubachko, S. Barilo, A. Sadovnikov, R. Pisarev, and A. Kalashnikova, Switching of an antiferromagnet controlled by spin canting in a laser-induced hidden phase, *Physical Review Letters* **135**, 266705 (2025).
- [56] C. Schönfeld, L. Feuerer, J. Bär, L. Dörfelt, M. Kerstingskötter, T. Dannegger, D. Wuhler, W. Belzig, U. Nowak, A. Leitenstorfer, *et al.*, Dynamical renormalization of the magnetic excitation spectrum via high-momentum nonlinear magnonics, *Science Advances* **11**, eadv4207 (2025).